Journal of ELECTRONIC MATERIALS, Vol. 46, No. 7, 2017
DOI: 10.1007/s11664-017-5503-z

Effect of Doping Materials on the Low-Level NO Gas Sensing Properties of ZnO Thin Films

TUGBA ÇORLU ,[1,4] IRMAK KARADUMAN,[1] MEMET ALI YILDIRIM,[2] AYTUNÇ ATEŞ,[3] and SELIM ACAR[1]

1.—Department of Physics, Science Faculty, Gazi University, Ankara, Turkey. 2.—Department of Electric Electronics Engineering, Engineering Faculty, Erzincan University, Erzincan, Turkey. 3.—Department of Material Engineering, Engineering and Natural Sciences Faculty, Yıldırım Beyazıt University, Ankara, Turkey. 4.—e-mail: tugbacorlu@gmail.com

In this study, undoped, Cu-doped, and Ni-doped ZnO thin films have been successfully prepared by successive ionic layer adsorption and reaction method. The structural, compositional, and morphological properties of the thin films are characterized by x-ray diffractometer, energy dispersive x-ray analysis (EDX), and scanning electron microscopy, respectively. Doping effects on the NO gas sensing properties of these thin films were investigated depending on gas concentration and operating temperature. Cu-doped ZnO thin film exhibited a higher gas response than undoped and Ni-doped ZnO thin film at the operating temperature range. The sensor with Cu-doped ZnO thin film gave faster responses and recovery speeds than other sensors, so that is significant for the convenient application of gas sensor. The response and recovery speeds could be associated with the effective electron transfer between the Cu-doped ZnO and the NO molecules.

Key words: Gas sensor, SILAR method, copper, nickel

INTRODUCTION

Breath analysis represents a promising non-invasive, fast, and cost-effective alternative to well-established diagnostic and monitoring techniques such as blood analysis, endoscopy, ultrasonic, and tomographic monitoring. Portable, non-invasive, and low-cost breath analysis devices are becoming increasingly desirable for monitoring different diseases, especially asthma. Because of this, NO gas sensing at low concentrations has attracted progressive attention for clinical analysis in asthma.[1–5]

Many types of semiconductor metal oxide gas sensors such as ZnO, SnO_2, NiO, CuO, and WO_3[6,7] have been shown to assist the gas detection process and have attracted the attention of several researchers due to their good reproducibility, better sensitivity, low cost, great stability, and features.[8] Among them, ZnO is a promising n-type semiconducting metal oxide, which exhibits remarkable properties such as being non-toxic, cost-effective, highly abundant in nature, and has a great variety of available forms (such as thin film and nanowires) and high chemical stability.[9]

Fabrication method is one of the important factors affecting sensor performance.[10] Many synthetic methods have been employed for the preparation of metal oxide semiconductors, including sol–gel processes, chemical spray pyrolysis, and SILAR.[11] Several research groups have reported different growth methods to produce ZnO composite films for gas sensor applications with different gases, but there are very few reports on NO gas sensing properties of ZnO nanostructure grown by SILAR method. Currently, the SILAR method is favorable and considered to be a chemical method capable of depositing a variety of compound materials in nanomaterial form for metal oxide gas sensors. SILAR technique is a good option due to its simplicity and low temperature of deposit onto thin films. It does not require high-quality substrates and can operate at room temperature without the need for vacuum. In addition, SILAR method

(Received November 19, 2016; accepted April 1, 2017; published online April 19, 2017)

provides optimal fabrication conditions to obtain high quality ZnO thin films. Stoichiometric precipitation can easily be obtained. Since the basic building materials are ions instead of atoms, the preparation parameters are easily controllable, and the best orientation and particle structure can be obtained at room temperature.[12]

The sensitivities of gas sensors can be enhanced through the formation of heterostructures by adding noble metals. The literature review clearly shows that the ZnO samples are used in gas sensing applications as a sensing material and the gas sensing properties of these samples are affected by the production method and doping materials.[13,14] Using this approach, room temperature gas sensing is also feasible.[14] Doping contents, distribution, and size of metallic or metal oxide catalysts are key parameters for enhancing gas selectivity, as well as sensitivity.[15] These materials, which differ according to production methods have started to be widely used in industrial areas. By manufacturing doping MOS structures, it is possible to develop more efficient sensor sensing layers.[15]

In this present work, we prepared ZnO, $Zn_{0.75}Cu_{0.25}O$ and $Zn_{0.75}Ni_{0.25}O$ thin films with using SILAR method. Gas sensing properties of these nanostructures towards to low level NO gas concentration are investigated as a function of Cu and Ni doping.

EXPERIMENTAL PROCEDURE

The thin films were prepared using SILAR method at room temperature and ambient pressure. In order to prepare ZnO, $Zn_{0.75}Cu_{0.25}O$, and $Zn_{0.75}Ni_{0.25}O$ thin films, aqueous zinc-ammonia complex ions ($[Zn(NH_3)_4]^{2+}$), aqueous copper-ammonia complex ions ($[Cu(NH_3)_4]^{2+}$), and aqueousnickel-ammonia complex ions ($[Ni(NH_3)_4]^{2+}$) were chosen for the cation precursors, in which analytical reagents of $ZnCl_2$ (%99) of 0.1 M, $CuCl_2$ (%99) of 0.1 M, $NiCl_2$ (%99) of 0.1 M, and concentrated ammonia (NH_3) (25–28%) were used. Double distilled water was used as a solvent and the molar ratio of Cu-Ni-Zn:NH_3 is 1:10 that obtained as a result of several experiments.[16] The obtained $[Zn(NH_3)_4]^{2+}$, $[Cu(NH_3)_4]^{2+}$, and $[Ni(NH_3)_4]^{2+}$ complexes were mixed in proper proportion according to the composition for ZnO, $Zn_{0.75}Cu_{0.25}O$ (CZO), and $Zn_{0.75}Ni_{0.25}O$ (NZO) thin films.

To prepare nanostructure thin films, one SILAR preparation cycle involves the four following steps: (1) immersing the substrate in the Cu-Ni-Zn species for 15 s (ZnO), 18 s (CZO), 25 s (NZO) to create a thin liquid film containing Zn, Cu-Zn, and Ni-Zn ammonia complex ions on the substrate, respectively; (2) immersing immediately the withdrawn substrates in hot water (~90°C) for 7 s to form ZnO, CZO, and NZO nanostructure layers; (3) drying the substrate in air for 60 s; and (4) rinsing the substrate in a separate beaker for 30 s (ZnO and CZO) and 20 s (NZO) to remove large and loosely bonded ZnO, CZO, and NZO particles. Thus, one SILAR cycle for nanostructure thin films preparation was completed, as shown in Fig. 1. The ZnO, CZO, and NZO nanostructure films were prepared by repeating 30 SILAR cycles.

To investigate doping materials effect on the structural, compositional and morphological properties of the thin films, XRD, EDX, and SEM measurements were analyzed. For structural, compositional, and morphological studies, PANalytical Empyrean x-ray diffractometer using CuKα (λ = 1.5405 Å) radiation and the FEI Quanta FEG 450 model SEM with energy dispersive x-ray analysis (EDS) attachment were used, respectively. The thickness of thin films was measured using a stylus ellipsometer system (J. A. Woolam Co, Inc., V-VASE). The thickness of ZnO, CZO, and NZO was measured to be 90 nm, 85 nm, and 97 nm, respectively.

The gas-sensing performance of the sensors were tested with a gas-sensing measurement system. The gas sensing measurement system working principle is given in our previous work.[17] The gas sensing measurements were carried out for NO gas at different concentrations from 100 ppb to 900 ppb and different operating temperatures between 35°C and 115°C with 10°C steps by monitoring the resistance changes. Dry air was used as the carrier gas which is % 99.999 purity (Dry air was the "blank" gas used to purge the sensor). The flow rate of the dry air undergoing testing was fixed at 500 cm^3/min during the measurements. Air flow rate, under the same conditions in order to observe the behavior of different concentrations must be kept always constant. Relative humidity was kept constant (about 25%) for all measurements, monitored by a Honeywell HIH-4000 humidity sensor. The NO concentration and dry airflow rates were controlled by computer controlled mass flow controllers (MKS Series). A LakeShore 325 temperature controller with platinum RTDs was used to maintain a constant temperature. The sensor resistance was continuously monitored with a computer controlled system by using a Keithley 2400 source meter and data was collected in real-time using a computer with corresponding data acquisition hardware and software. Before the measurements, sensors under test were fixed into chamber and the samples are kept constant at 130°C for 20 min in order to enhance the adhesion.

RESULTS AND DISCUSSION

The crystal structure of ZnO, CZO, and NZO thin films was analyzed by XRD measurements at room temperature. The XRD patterns of the thin films are shown in Fig. 2. All the thin films have polycrystalline structure with orientation along with different planes (Fig. 2).The undoped ZnO thin film has (100), (101), and (102) planes, which belong to the

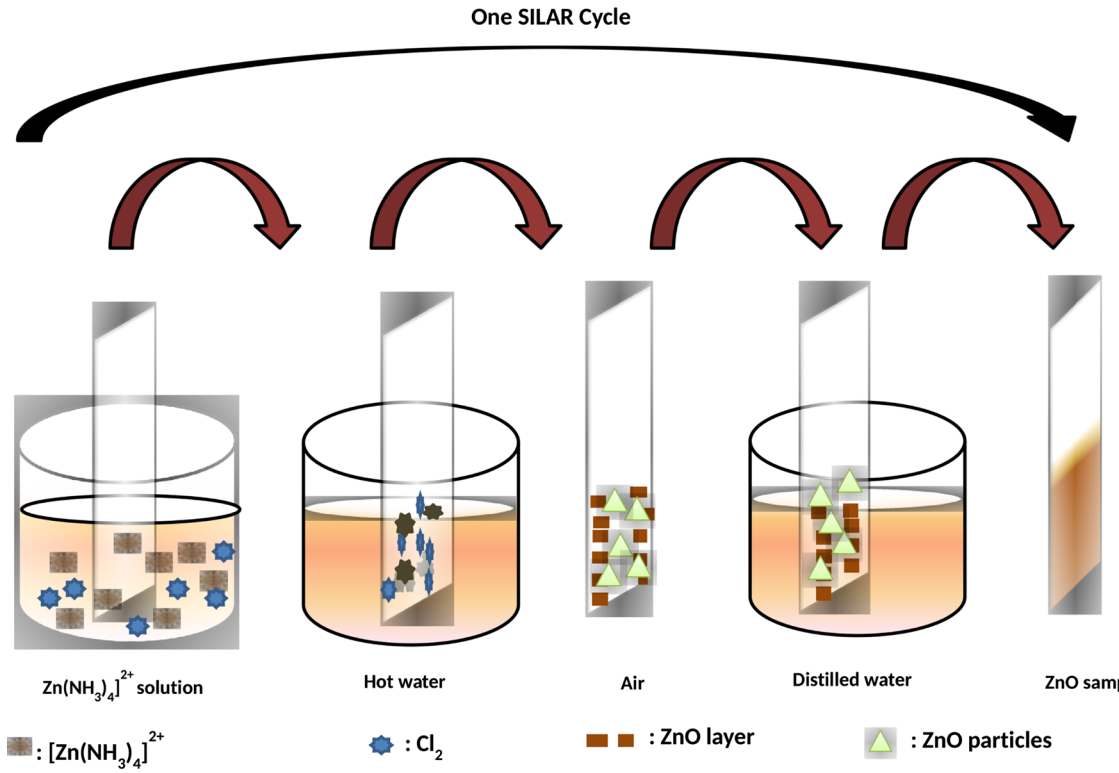

Fig. 1. One deposition cycle of thin film by SILAR method.

hexagonal wurtzite phase (JPCDS Card No: 36-1451).[18,19] It is clearly observed in XRD patterns that the NZO and CZO thin films have both ZnO phase and secondary phases, namely NiO and CuO phases, respectively. In addition, no peaks for any impurities such as Ni or Cu are observed in the XRD patterns. In NZO thin film, a new peak that corresponds to the (200) diffraction of cubic NiO phase (JPCDS Card No:47-1049) is appeared with Ni doping. Similarly in CZO thin film, two new peaks that correspond to the (111) and (200) diffractions of monoclinic CuO phase (JPCDS Card No: 80-1916) appear with Cu doping. However, as seen in the XRD patterns, all thin films show a strong diffraction peak corresponding to the (101) diffraction of hexagonal wurtzite ZnO phase. As the intensity of the characteristic peaks of ZnO phase decreases, the (102) peak disappears, and the crystal quality of the thin films deteriorate with Ni, Cu doping.

The surface morphology of the thin films as sensor materials influences their electrical properties. Thus, it is very crucial to characterize the surface morphology of the thin films. The morphology images of ZnO, CZO, and NZO thin films are given in Fig. 3a, b, and c. Figrue 3a shows the SEM image of the undoped ZnO, which presents a dense, well-grown flower-like and homogenous structure. These SEM images show that crystallization quality and surface morphology of the thin films are changed with the doped materials. Fig 3b shows surface

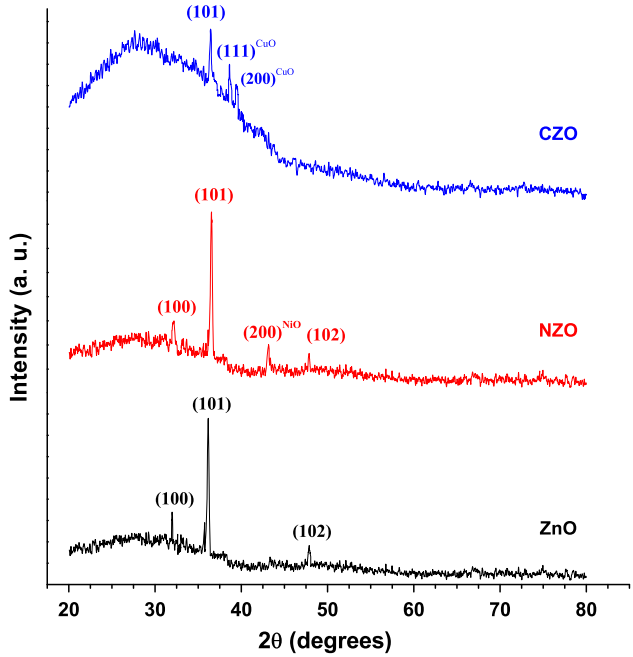

Fig. 2. XRD patterns of ZnO, CZO, and NZO thin films.

morphology of the CZO. The CZO thin film is composed of a nanorod structure belonging to the ZnO phase and CuO phase formed around it. The surface morphology of ZnO changes from a flower-like structure to a nanorod structure with Cu

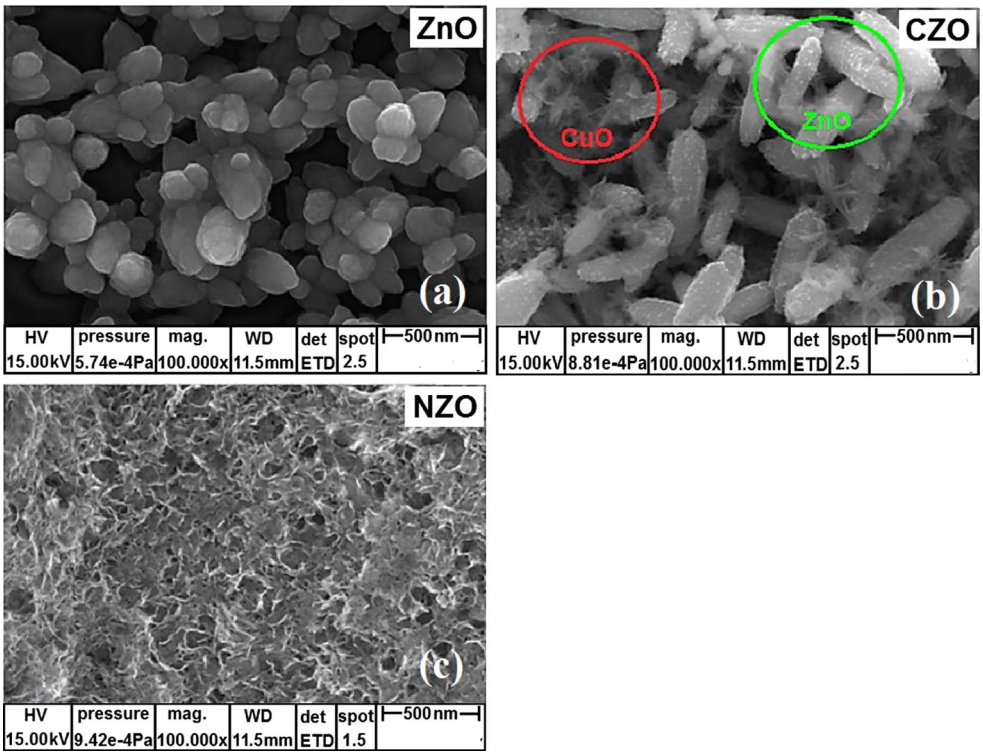

Fig. 3. SEM images of ZnO (a), CZO (b), and NZO (c) thin films.

doping. However, the NZO includes no flower-like or nanorod structures with Ni doping (Fig. 3c). The SEM image of the NZO reveals that the surface has porous and some overgrown clusters. Consequently, the Cu and Ni doping process changes significantly the surface properties of the ZnO.

The compositional analysis of ZnO, CZO, and NZO thin films is performed by energy dispersive x-ray analysis (EDS). Fig 4 shows EDX spectra of ZnO, CZO, and NZO thin films. EDS analysis shows the presence of Zn, Cu, Ni, and O elements in the thin films (Fig. 4). The atomic percent values of these elements in the thin films are given in the inset of EDS spectras (Fig. 3). The presence of Si and Ca elements in the spectra may originate from the substrate. The atomic ratios (at.%) of Cu and Ni in the ZnO nanostructure are approximately the same as the initial ratio.

The gas response of a semiconductor sensor is greatly affected by the operating temperature, which results from the effect of temperature on adsorption/desorption and surface reaction of gas.[20] The sensing characteristics of the films towards NO gas at different working temperatures were analyzed. Fig 5 shows the response of ZnO, CZO, and NZO for 900 ppb NO gas as a function of operating temperature from 35°C to 115°C. Responses increase rapidly and reach the maximum value at 85°C and then decrease as the temperature is further increased. Because sufficient thermal energy is essential to overcome the activation energy barrier of oxygen chemisorption and surface reaction at temperature range from 35°C to 85°C, once the operating temperature over 85°C, the amount of desorbed gas will increase, leading to the reduce of response. Because of adsorption and desorption of gas molecules on the sensors' surface, the change of response can be observed. As seen, the maximum responses of all sensors are found at 85°C.

Fig 6a shows the dynamic responses of the sensors to NO with the different concentrations of from 100 ppb to 900 ppb at the optimal temperature of 85°C. Accordingly, the response of the sensor undergoes an increase as it is exposed to NO and a decrease as air is introduced back into the testing chamber, based on the electric circuit of the gas sensing test system. The results are repeatable for all ppb levels. Figure 6b depicts the response of sensors versus gas concentrations. The responses of doped sensors increase gradually with the increasing of NO gas concentration compared to ZnO. There was no acceptable response observed for ZnO sensors in this working gas concentration range. The increase in the sensing response with the gas concentration is due to increase in the probability of adsorption of gas molecules at the active sites on sensing layers.[21]

It is clearly seen from Fig. 6a and b that NZO and CZO sensors have almost similar responses at low concentrations of NO gas and they exhibited six times higher response compared with ZnO. Above 300 ppb, CZO became more sensitive then NZO; however, there was still no acceptable response observed for ZnO. The responses were calculated to

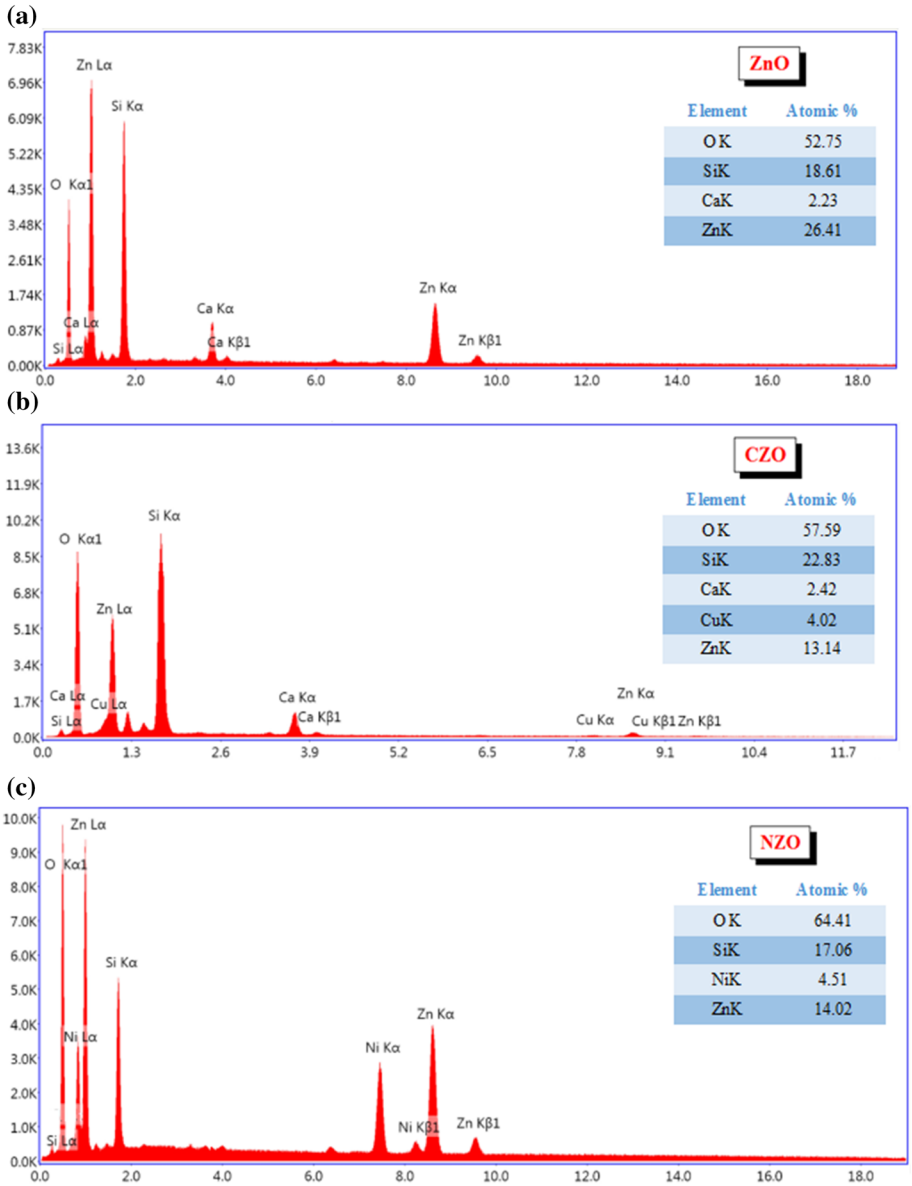

Fig. 4. EDAX analysis of ZnO (a), CZO (b), and NZO (c) thin films.

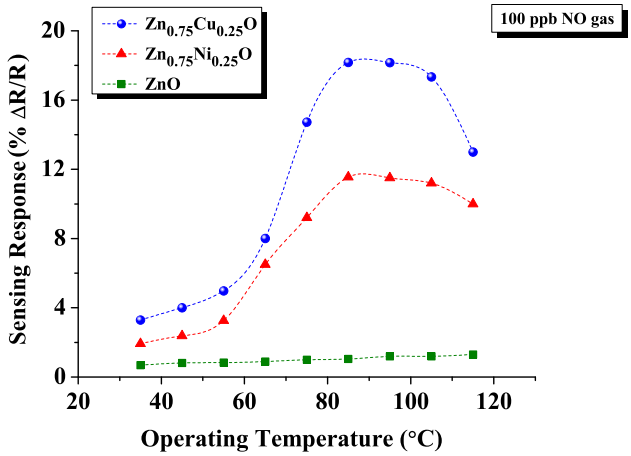

Fig. 5. The responses of ZnO, CZO, and NZO thin films to 100 ppb NO gas as a function of temperature.

be 1%, 11%, and 18% for ZnO, NZO, and CZO, respectively, at 900 ppb NO gas concentration. The CZO sensor shows the best dynamic gas sensing behaviors. Therefore, detailed investigations about the sensor properties were carried out only for CZO.

Figure 7 indicates the time dependence of the sensitivity in measurement process. Figrue 7a shows only one peak to determine the response and recovery times of sensor. The response and recovery times were calculated as the times to reach 90% of the resistance change above exposure to NO and air, respectively. The response time was calculated at 25 s and the recovery time was calculated at 34 s for 100 ppb NO gas concentrations. Figure 7b shows the response and recovery times for all NO gas concentrations. The CZO sensor exhibited fast response times compared to recovery times. The

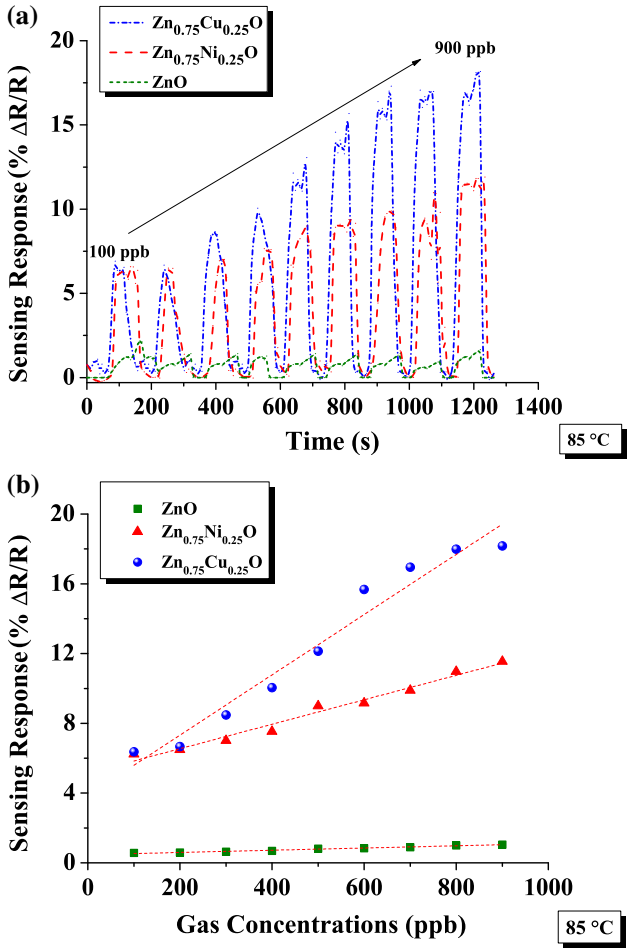

Fig. 6. (a) The dynamic gas responses as a function of time to different NO concentrations from 100 ppb to 900 ppm at 85°C for ZnO, CZO, and NZO thin films. (b) The responses as a function of gas concentrations to different NO concentrations from 100 ppb to 900 ppb at 85°C for ZnO, CZO, and NZO thin films.

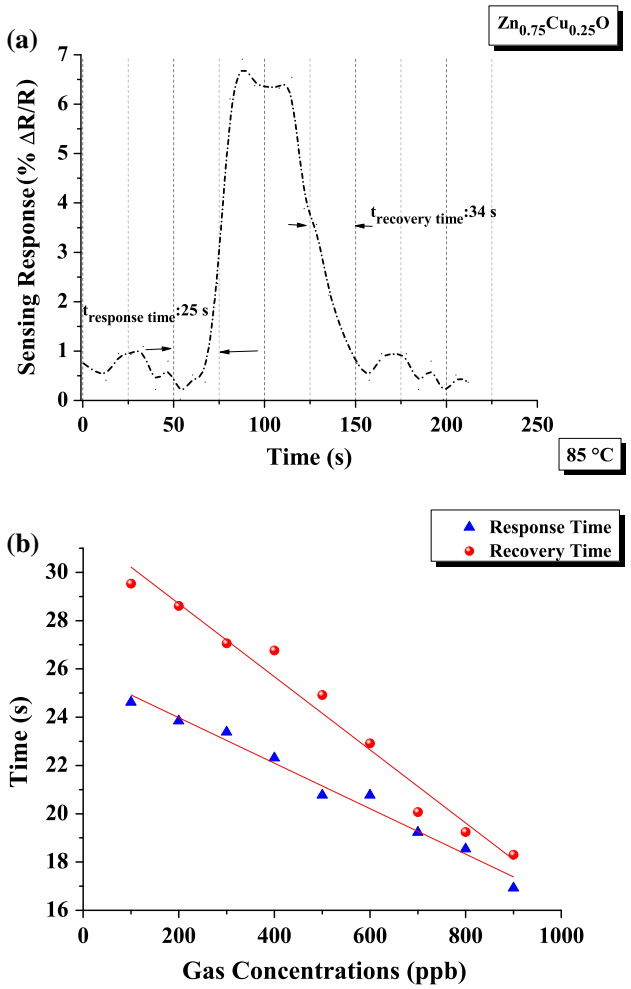

Fig. 7. (a) The response and recovery time for 100 ppb NO gas concentration for CZO thin film. (b) The response and recovery times for different NO gas concentrations from 100 ppb to 900 ppb for CZO thin films.

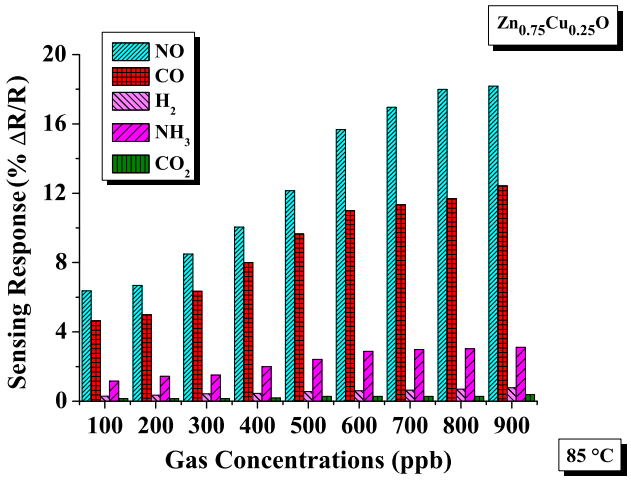

Fig. 8. The selectivity measurements for CZO thin film..

response and recovery times are optimized by oxygen vacancies, which supply further active center for reactions.

It is well known that the high selectivity is an important factor for a reliable sensor. Figure 8 depicts the selectivity measurements of CZO sensor to NO, CO, NH_3, H_2, CO_2 gases. Under the operating conditions, our sensor demonstrated selective sensing to NO gas. Its response values for 900 ppb are about 18%, 12%, 3%, 0.8%, and 0.4% for NO, CO, NH_3, H_2, CO_2 gases, respectively. It can be seen that the sensor exhibited good selectivity to NO gas. The good sensing performance is attributed to its native nature, and in particular the high surface area, which enables a large exposure of surface atoms to provide more active sites for the absorption of gas molecules and hence facilitate the surface reactions.

Gas sensing mechanism belongs to surface controlled mechanism, i.e. resistance change is controlled by the surface area and amount of chemisorbed oxygen. The atmospheric oxygen species adsorbed on the surface of the samples capture electrons from the conduction band creating a depletion region in the samples. The electron

transfer from the conduction band to the adsorbed oxygen species, O^-_{ads} or $2O^-_{ads}$ will then proceed as follows[22]:

$$O_{2(ads)} + e^- \leftrightarrow 2O^-_{ads} \quad (1)$$

The reaction between the electron and the chemisorbed oxygen results in a decrease in the electron concentration at the surface of the samples. Therefore, when the samples are exposed to NO gas, they react with the chemisorbed oxygen[23]:

$$NO + e^- \leftrightarrow NO_2 \quad (2)$$

As a consequence, a rapid increase in the resistance of the film with time up to stabilization was observed. Moreover, the examination of the direction of change in resistance shows that these films exhibit *n*-type character because the resistance increased under NO gas.[23]

For Cu-doped ZnO, the stability of the Coulomb forces of the interactions between the acceptor defects (CuZn) and intrinsic ZnO donors, namely, zinc interstitials or oxygen vacancies (Zn_i or V_O) can occur by the capture of an electron from the lattice. A model of an associate donor–acceptor for CuZn was proposed by West et al.[24];

$$Cu^+_{Zn}(3d^{10}) + Zn^+_i(4s^1) \rightarrow \{[Cu]Zn^+_i(4s^1)\} \quad (3)$$

in the Kröger–Vink notation

$$Cu^*_{Zn} + Zn^*_i \rightarrow [Cu_{zn} - Zn_i]^x \quad (4)$$

The surface potential barrier for electrons in the conduction band can be increased by the created complex defects in Cu-doped ZnO. In general, the amount of adsorbed oxygen species on the surface would depend on the Cu atoms in the ZnO, which in turn would oxidize the exposed gas. Eventually, while the Cu concentration on the ZnO surface increases, it leads to a higher response due to the increase in the amount of adsorbed oxygen on the film surface.[23–25]

In other words, the Cu atoms are weakly bonded with the oxygen atoms, the resulting complex is readily dissociated at relatively low temperature, and the oxygen atoms are produced. The created atoms migrate along the surface of the grains. This migration is induced by the catalyst atoms and is known as spillover of the gas ions. The oxygen atoms capture electrons from the surface layer and acceptor surface states are formed. As a result, this amount of Cu doping would also be sufficient to promote the catalytic reaction effectively and the overall change in the resistance on the exposure of NO gas leading to an increase in the sensitivity. When the amount of Cu is less than the optimum, the surface dispersion may be poor and the sensitivity of the film is observed to be decreased since the amount may not be sufficient to promote the reaction more effectively.[25]

Surface morphology also has an impact on the gas adsorption, because the effective surface area or contact area of ZnO increases sensitivity as it is suitable for gas adsorption.[25] For this reason, it is anticipated that adaptation of the effective surface area may lead to a significant improvement in sensitivity.[25]

CONCLUSION

In this study, ZnO, CZO, and NZO thin films were successfully prepared by SILAR method at room temperature for fabrication of highly sensitive NO gas sensors. The advantages of this method are its simplicity, low cost, non-vacuum system, and fast growth rate, etc. The XRD measurements of thin films indicated that undoped ZnO has only hexagonal wurtzite single phase, CZO and NZO also have a secondary phase, namely a monoclinic CuO phase and cubic NiO phase, respectively. The surface morphology of ZnO changes from a flower-like structure to a nanorod structure with Cu doping and from a flower-like structure to a porous and cluster structure with Ni doping. The possible sensing mechanism and the relationship between the doping material and the sensing surface were proposed. The sensor with copper doped to ZnO thin film showed a better sensor characteristics to NO. This may be related to the catalytic effect of Cu and also the morphology of CZO thin film. The results demonstrate that the copper doped ZnO sensor is a promising candidate for nitric oxide gas sensor, which can be used in the medical industry for breath analysis.

ACKNOWLEDGEMENTS

This work is supported by TUBITAK Project No: 115M658 and Gazi University Scientific Research Fund Project No: 05/2015-09.

REFERENCES

1. N. Docquier and S. Candel, *Prog. Energy Combust. Sci.* 28, 107 (2002).
2. S.P. Mondal, P.K. Dutta, G.W. Hunter, B.J. Ward, D. Laskowski, and R.A. Dweik, *Sens. Actuators B* 158, 292 (2011).
3. G.W. Hunter, J.C. Xu, A.M. Biaggi-Labiosa, D. Laskowski, P.K. Dutta, S.P. Mondal, B.J. Ward, D.B. Makel, C.C. Liu, C.W. Chang, and R.A. Dweik, *J. Breath Res.* 5, 037111 (2011).
4. A.D. Smith and N. Engl, *J. Med.* 352, 2163 (2005).
5. N.M. Grob and R.A. Dweik, *J. Breath Res.* 2, 037002 (2008).
6. K.G. Girija, K. Somasundaram, A. Topkar, and R.K. Vatsa, *J. Alloy Compd.* 684, 15 (2016).
7. L. Wang, Y. Wang, K. Yu, S. Wang, Y. Zhang, and C. Wei, *Sens. Actuators B* 232, 91 (2016).
8. S.C. Navale, V. Ravia, I.S. Mulla, S.W. Gosaviand, and S.K. Kulkarni, *Sens. Actuators B* 126, 382 (2007).
9. V. Galstyann, E. Comini, C. Baratto, G. Faglia, and G. Sberveglieri, *Ceram. Int.* 41, 14239 (2015).
10. D.C. Joshi, K. Dasari, S. Nayak, R. Palai, P. Suresh, and S. Thota, *J. Electron. Mater.* 45, 2059 (2016). doi: 10.1007/s11664-015-4243-1.

11. R.R. Salunkhe and C.D. Lokhande, *Sens. Actuators B* 129, 345 (2008).
12. M.A. Yıldırım, S.T. Yıldırım, E.F. Sakar, and A. Ates, *Spectrochim. Acta Part A Mol. Biomol. Spectrosc.* 133, 60 (2014).
13. G.H. Mhlongo, K. Shingange, Z.P. Tshabalala, B.P. Dhonge, F.A. Mahmoud, B.W. Mwakikunga, and D.E. Motaung, *Appl. Surf. Sci.* 390, 804 (2016).
14. L.-Y. Hong, H.-W. Ke, C.-E. Tsai, and H.-N. Lin, *Mater. Lett.* 185, 243 (2016).
15. S. Xu, J. Gao, L. Wang, K. Kan, Y. Xie, P. Shen, L. Li, and K. Shi, *Nanoscale* 7, 14643 (2015).
16. M.A. Yıldırım, Y. Akaltun, and A. Ates, *Solid State Sci.* 141, 1282 (2012).
17. I. Karaduman, O. Barin, M. Ozer, and S. Acar, *J. Electron. Mater.* 45, 3914 (2016). doi:10.1007/s11664-016-4480-y.
18. D.L. Hou, X.J. Ye, H.J. Meng, H.J. Zhou, X.L. Li, C.M. Zhen, and G.D. Tang, *Appl. Phys. Lett.* 90, 142502 (2007).
19. E. Amoupour, A. AbdolahzadehZiabari, H. Andarva, and F.E. Ghodsi, *Superlattices Microstruct.* 65, 332 (2014).
20. N. Nİthyavathy, S. Arunmetha, M. Vinoth, G. Sriram, and V. Rajendran, *J. Electron. Mater.* 45, 4 (2016).
21. J. Wang, L. Wei, L. Zhang, J. Zhang, H. Wei, C. Jiang, and Y. Zhang, *J. Mater. Chem.* 22, 20038 (2012).
22. H. Gómez-Pozos, E.J.L. Arredondo, A.M. Álvarez, R. Biswal, Y. Kudriavtsev, J.V. Pérez, Y.L. Casallas-Moreno, and M.D.L.L. Olvera Amador, *Materials* 9, 87 (2016).
23. L.P. Chikhale, J.Y. Patil, A.V. Rajgure, R.C. Pawar, I.S. Mulla, and S.S. Suryavanshi, *J. Alloy Compd.* 608, 133 (2014).
24. C. West, D.J. Robbins, P.J. Dean, and W. Hays, *Phys. B C* 116, 492 (1983).
25. F.A. Kröger and H.J. Vink, *Solid State Phys.* 3, 307 (1956).